Letter to the Editor

No asymmetric outflows from Sagittarius A* during the pericenter passage of the gas cloud G2

J.-H. Park¹, S. Trippe^{*1}, T. P. Krichbaum², J.-Y. Kim¹, M. Kino³, A. Bertarini^{2,4}, M. Bremer⁵, and P. de Vicente⁶

- Department of Physics and Astronomy, Seoul National University, 1 Gwanak-ro, Gwanak-gu, Seoul 151-742, Korea e-mail: jhpark@astro.snu.ac.kr, trippe@astro.snu.ac.kr
- Max-Planck-Institut für Radioastronomie (MPIfR), Auf dem Hügel 69, 53121 Bonn, Germany
- Korea Astronomy and Space Science Institute (KASI), 776 Daedeokdae-ro, Yuseong-gu, Daejeon 305-348, Korea
- Institute of Geodesy and Geoinformation, Bonn University, Nussallee 17, 53115 Bonn, Germany
- Institut de Radioastronomie Millimétrique (IRAM), 300 rue de la Piscine, 38406 Saint-Martin d'Hères, France
- Observatorio Astronomico Nacional (IGN), Observatorio de Yebes, Aptdo. 148, Yebes, 19080 Guadalajara, Spain

ABSTRACT

The gas cloud G2 falling toward Sagittarius A* (Sgr A*), the supermassive black hole at the center of the Milky Way, is supposed to provide valuable information on the physics of accretion flows and the environment of the black hole. We observed Sgr A* with four European stations of the Global Millimeter Very Long Baseline Interferometry Array (GMVA) at 86 GHz on 1 October 2013 when parts of G2 had already passed the pericenter. We searched for possible transient asymmetric structure - such as jets or winds from hot accretion flows - around Sgr A* caused by accretion of material from G2. The interferometric closure phases remained zero within errors during the observation time. We thus conclude that Sgr A* did not show significant asymmetric (in the observer frame) outflows in late 2013. Using simulations, we constrain the size of the outflows that we could have missed to ≈ 2.5 mas along the major axis, ≈0.4 mas along the minor axis of the beam, corresponding to approximately 232 and 35 Schwarzschild radii, respectively; we thus probe spatial scales on which the jets of radio galaxies are suspected to convert magnetic into kinetic energy. As probably less than 0.2 Jy of the flux from Sgr A* can be attributed to accretion from G2, one finds an effective accretion rate $\eta \dot{M} \lesssim 1.5 \times 10^9 \text{ kg s}^{-1} \approx 7.7 \times 10^{-9} M_{\oplus} \text{ yr}^{-1}$ for material from G2. Exploiting the kinetic jet power–accretion power relation of radio galaxies, one finds that the rate of accretion of matter that ends up in jets is limited to $\dot{M} \lesssim 10^{17} \, \mathrm{kg \, s^{-1}} \approx 0.5 M_{\oplus} \, \mathrm{yr^{-1}}$, less than about 20% of the mass of G2. Accordingly, G2 appears to be largely stable against loss of angular momentum and subsequent (partial)

Key words. accretion, accretion disks — black hole physics — Galaxy: center — radio continuum: general

Narayan et al. 1998 and references therein). Sgr A* shows a slightly inverted radio spectrum peaking at mm-to-submm wavelengths (Zylka et al. 1992; Falcke et al. 1998; Melia & Falcke 2001; Bower et al. 2015).

The emission mechanism of Sgr A* is a matter of ongoing debate. On the one hand, radiatively inefficient accretion flows (RIAFs; e.g., Yuan et al. 2003) reproduce the observed fluxes at various wavelengths successfully. On the other hand, multiple studies (Falcke, & Markoff 2000; Markoff et al. 2001; Yuan et al. 2002; Markoff et al. 2007; Falcke et al. 2009) have pointed out the need for parts of the emission to originate

from jets, as well as observational evidence for the presence of jets (Yusef-Zadeh et al. 2012; Li, Morris & Baganoff 2013). The current lack of structural information for Sgr A* prevents an unambiguous decision between competing theories. At the shortwavelength side of the submm-bump, where the emission becomes optically thin, instruments with the necessary spatial resolution are not available. At wavelengths of more than a few millimeters, the source structure is washed out by interstellar scattering (e.g., Bower et al. 2006). Lu et al. (2011) found evidence that the shape and orientation of the elliptical Gaussian changes with frequency; this could be interpreted as an intrinsic structure which is slightly misaligned with the scattering disk, shining through towards higher frequencies. In addition, recent Very Long Baseline Interferometry (VLBI) observations at 43 GHz have been able to resolve an intrinsic elliptical structure with a preferred geometrical axis (Bower et al. 2014). This structure might indicate an existence of jets but could also be the result of an elongated accretion flow such as a black hole crescent (e.g., Kamruddin, & Dexter 2013).

Recently, a gas cloud labeled G2 was observed to move toward Sgr A* on a nearly radial orbit (Gillessen et al. 2012). As yet, two possible structures of G2 have been discussed mainly, with the first scenario being that G2 is a localized over-dense region within an extended gas streamer. This is in agreement with

^{*} Corresponding author

observations reporting that G2 is composed of a compact head and a more widespread tail (Gillessen et al. 2013b; Pfuhl et al. 2015). The two components are on approximately the same orbit and connected by a faint bridge in position-velocity diagrams, indicating that they might share the same origin. According to this scenario, the pericenter passage started in early 2013 (Gillessen et al. 2013a) and lasted over one year while G2 has been stretched substantially along its orbit by tidal shearing caused by the gravitational potential of Sgr A* (Pfuhl et al. 2015). Test particle simulations have provided a good explanation on the dynamics of G2, corresponding that hydrodynamic effects have not been significant (e.g., Pfuhl et al. 2015; see also Schartmann et al. 2012). The second possibility under discussion is that G2 is a circumstellar cloud around a star which provides stabilizing gravity and replenishes gas continuously. Studies supporting this scenario pay attention to the possibility that the tail is just a fore/background feature and not physically connected to G2 (Phifer et al. 2013; Valencia-S., et al. 2015). Recent observations also have shown that G2 survived its pericenter passage as a compact source, which might be a clue for G2 being a star enshrouded by gas and/or dust (Witzel et al. 2014; Valencia-S., et al. 2015). This scenario was modeled analytically (Miralda-Escudé 2012; Scoville & Burkert 2013) and explored with the help of numerical simulations (Ballone et al. 2013; De Colle et al. 2014; Zajaček et al. 2014).

Interactions with the accretion flows toward Sgr A* might cause G2 to lose angular momentum, resulting in parts of it to be accreted by the black hole (Anninos et al. 2012; Burkert et al. 2012; Schartmann et al. 2012). Accordingly, one may expect an increased radio luminosity (e.g., Mahadevan 1997; Mościbrodzka et al. 2012) as well as an increase in source size (e.g., Mościbrodzka et al. 2012). In addition, radiobright outflows, like jets or wind-like outflows related to RIAFs (Yuan et al. 2003; Mościbrodzka et al. 2012; Liu & Wu 2013), might become observable on spatial scales of ≤ 1 mas. In order to search for such transient structure, we performed VLBI observations with four European stations of the Global Millimeter VLBI Array (GMVA) at 86 GHz, providing an angular resolution down to ≈ 0.3 mas. Our observing frequency of 86 GHz is in a region where scattering vanishes and dominates less the images of Sgr A* at frequencies less than about 43 GHz (Bower et al. 2004, 2006; Shen et al. 2005).

2. Observations and Data Analysis

We observed Sgr A* at 86 GHz on 1 October 2013 using four GMVA stations of the European VLBI Network (EVN): Effelsberg (EF), Pico Veleta (PV), Plateau de Bure (PB), and Yebes (YS). A combination of low declination of Sgr A^* (-29°), high latitude of the stations (the minimum latitude being 37° for Pico Veleta), and a technical problem at Yebes station limited our observing times to around 1.5 hours for Yebes and 2.5 hours for the other stations. We observed both circular polarizations except of Yebes station where only left circular polarization (LCP) data were obtained. The data were recorded with the Mark 5 VLBI system (2-bit sampling) using the digital baseband converter (DBBC) in polyphase filter bank mode with a bandwidth of 32 channels, each 16 MHz wide (total bandwidth 512 MHz). All data were correlated with the DifX VLBI correlator of the MPIfR (Bonn, Germany). Our calibrators (fringe finding sources) were NRAO 530 and 1633+38.

We followed the standard procedures for initial phase and amplitude calibration using the AIPS software package (Greisen 2003) and applied phase self-calibration using the Caltech

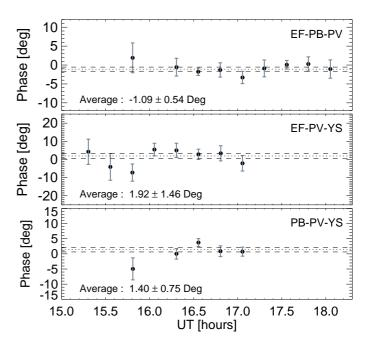


Fig. 1. Closure phases vs. time for three independent VLBI triangles. Each data point denotes a closure phase measurement averaged over one scan of 6 minutes; error bars correspond to 1σ errors. Dotted lines indicate weighted averages of all data points, dashed lines represent the corresponding standard errors of mean. Average phase values are noted in each diagram. Phases for the triangle EF-PB-PV are extracted from Stokes I data, phases for the other triangles are from LL data.

Difmap package (Shepherd 1997) with a point-source model. The geometry of our observation resulted in a very elongated beam (point spread function) with full widths at half maximum (FWHM) of 3.02 mas and 0.33 mas, respectively, at a position angle of -22° . For the flux density of Sgr A* we found a value of $\approx 1.4 \pm 0.3$ Jy).

We used the evolution of *closure phases* to search for asymmetric, extended emission around Sgr A*. A closure phase is the sum of the interferometric phases of the three baselines in a closed triangle of stations; it is free from antenna-based phase errors (e.g., Thompson et al. 2001). The closure phase for a centrally symmetric brightness distribution is zero. The amount of deviation from zero and the time scales of fluctuations of the closure phases can be used to probe the structure of an asymmetric source even if it cannot be imaged (due to lack of flux or insufficient *uv* plane coverage). This technique was already used by Krichbaum et al. (2006) and Lu et al. (2011) who found the closure phases of Sgr A* to be consistent with zero throughout their observations in October 2005 and May 2007, respectively.

We extracted the closure phases from the visibility data for three independent triangles of VLBI stations, initially binned into 10-second time bins. We flagged data with large errors (larger than the standard deviation of the data for a given triangle) and obvious outliers. The fraction of flagged data is 8.9%, 7.9%, and 6.0% for the triangles of EF-PB-PV, EF-PV-YS, and PB-PV-YS, respectively; the difference between the results obtained with and without flagging is insignificant however. We took the weighted average of the remaining values for each scan of 6 minutes; the resulting data set is shown in Fig. 1. We obtained a combined reduced χ^2 value of 1.34 for all the closure phases for all the independent triangles based on the null hypothesis "the closure phase is zero all the time". The corresponding false alarm probability (p-value) is 0.136; this value is clearly too

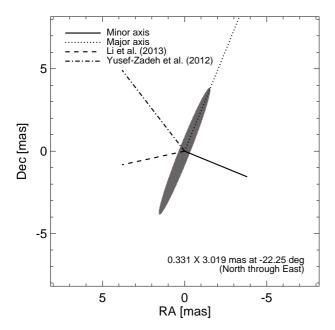


Fig. 2. Outflow orientations assumed in our simulation. The gray ellipse (with FWHM and position angle as noted) indicates the beam, dashed lines indicate four outflow orientations: along the major axis, along the minor axis, along the jet direction claimed by Li, Morris & Baganoff (2013), and along the one claimed by Yusef-Zadeh et al. (2012).

high to reject the null hypothesis (this outcome did not change when choosing bin sizes other than 6 min). Consequentially, we conclude that the closure phases are in agreement with zero during the observing time.

3. Discussion

The absence of a deviation of the closure phases from zero — within typical errors of a few degrees — implies the absence of asymmetric structure around Sgr A* at the time of our observation. A priori, bipolar, symmetric jets can account for zero closure phases. However, if the jet axis is oriented partially along the line of sight, the flux observed from the jet approaching the observer (f_+) is amplified while that from the receding jet (f_-) is dimmed by the Doppler effect. If the jets on both sides of the black hole have the same luminosity intrinsically, the observed ratio of the two fluxes is

$$\frac{f_{+}}{f_{-}} = \left(\frac{1 + \beta \cos \theta}{1 - \beta \cos \theta}\right)^{2 + \alpha} \tag{1}$$

(e.g., Beckmann & Shrader 2012), where β is the jet speed in units of speed of light, θ is the angle between the jet axis and the line of sight, and α is the spectral index defined via the flux density $S_{\nu} \propto \nu^{\alpha}$. Various observational constraints ($\alpha \approx 0.5$, $\beta \lesssim 0.1$; Lu et al. 2011) and model predictions for transient jets ($\theta \approx 60^{\circ}$, $\beta \approx 0.7$; Falcke et al. 1998, 2009) place the flux ratios to be expected anywhere between ≈ 1 and ≈ 6 . Accordingly, even intrinsically symmetric jets from Sgr A* might appear asymmetric in the observer frame.

In order to constrain the size of outflows that we could have missed, we performed simple simulations. We placed artificial, uni-polar secondary sources next to a primary point source model representing Sgr A* and compared the closure phases obtained from the resulting artificial visibility data with the observations. We considered two geometries: a single point source and

a jet composed of 10 equally spaced point sources (knots) with equal fluxes. We probed four orientations for the simulated outflows (See Fig. 2): along the major axis, along the minor axis of the beam, the jet direction claimed by Li, Morris & Baganoff (2013), and the jet direction claimed by Yusef-Zadeh et al. (2012). We used total fluxes of 0.2 Jy and 0.55 Jy for the artificial sources; these values ensure that our simulated outflows are sufficiently faint to not violate the constraints given by the known recent brightness evolution of Sgr A* (0.2 Jy from the mean variability of ≈15% from June 2013 to February 2014 at 41 GHz, with 0.55 Jy corresponding to the maximum variation in the same period (Chandler & Sjouwerman 2014)). For each simulation setup, we measured the average of absolute values of the closure phases for each triangle. We varied the distances of the model sources (in case of the jet model: the maximum distance) from Sgr A* until we found a critical distance at which the absolute values of the simulated closure phases exceeded those of the observations by more than the 1σ error at all triangles. We summarized our results in Table 1. Unsurprisingly, critical distances are smaller for brighter outflows. Jet-like structures lead to larger critical distances than equally luminous single, compact sources. As a consequence of the very elongated beam, the critical distances for sources located along the major axis of the beam are larger by a factor of \approx 7 than for those located along the minor axis. In a few cases (denoted 'N/A' in Table 1), the absolute values of the simulated closure phases were comparable to those of the observations for all distances of the model sources, meaning we could not identify a critical distance. Overall, our observations limit the extension of asymmetric (in the observer frame) jet-like outflows from Sgr A* to projected distances of ≈ 2.5 mas along the major axis and ≈ 0.4 mas along the minor axis.

Our analysis limits the (projected) extension of linear outflows to about 232 and 35 Schwarzschild radii, respectively, for outflows with fluxes of about 0.2 Jy; obviously, outflows substantially fainter could be larger and still remain undetected. Unfortunately, the resolution of our observations is not sufficient to probe structures in accretion flows expected to occur on scales $10R_{\rm S}$ (cf., e.g., Broderick et al. 2011); those observations will probably have to await the Event Horizon Telescope (cf. Fish et al. 2014). When referring to radio galaxies for comparison, especially to M 87 which has a central black hole with small angular diameter ($\approx 10 \,\mu as$) second only to Sgr A*, one notes that a distance of tens of Schwarzschild radii appears to be critical for the formation of AGN jets. Recent VLBI observations of the jet of M 87 find a transition in the collimation geometry at a distance of about $100 R_S$, with the jet opening angle being smaller outside this boundary; this has been interpreted as $\approx 100 R_S$ being the characteristic distance for the conversion of magnetic to kinetic energy in a magnetically launched jet (Hada et al. 2013). Accordingly, Sgr A* is potentially a very important test case for AGN jet physics if a jet is ever detected.

Our non-detection of outflows is consistent with earlier null results from VLBI observations of Sgr A* at 86 GHz (Krichbaum et al. 1998; Lo et al. 1998; Shen et al. 2005; Lu et al. 2011) despite the fact that we observed Sgr A* at an epoch of potentially increased accretion. Our results are in line with other recent observations finding that Sgr A* has been quiescent from radio to X-rays in 2013 and 2014 (Akiyama et al. 2013; Brunthaler & Falcke 2013; Chandler & Sjouwerman 2014; Degenaar et al. 2014). In addition, the zero closure phases within errors can put some constraints on the substructure in scattering disks of Sgr A* (e.g., Gwinn et al. 2014); this substructure must remain symmetric on

Table 1. Size constraints for outflows from Sgr A*.

		Minor axis		Major axis		Li+ 2013		YZ+ 2012	
	Triangle	0.2 Jy	0.55 Jy	0.2 Jy	0.55 Jy	0.2 Jy	0.55 Jy	0.2 Jy	0.55 Jy
Point source	EF-PB-PV	0.22 [21]	0.19 [18]	1.21 [114]	1.10 [104]	0.44 [41]	0.39 [36]	0.22 [20]	0.19 [18]
	EF-PB-YS	0.22 [21]	0.19 [18]	1.85 [174]	1.62 [152]	N/A	0.56 [52]	0.22 [20]	0.19 [18]
	PB-PV-YS	0.24 [22]	0.21 [20]	1.66 [156]	1.51 [142]	0.59 [55]	0.47 [44]	0.23 [22]	0.21 [20]
	Average	0.23 [21]	0.20 [19]	1.57 [148]	1.41 [133]	0.51 [48]	0.47 [44]	0.22 [21]	0.20 [18]
KNOTTY JET	EF-PB-PV	0.36 [34]	0.28 [26]	1.84 [173]	1.52 [143]	0.67 [63]	0.54 [51]	0.35 [33]	0.27 [25]
	EF-PB-YS	0.39 [36]	0.28 [26]	2.97 [279]	2.32 [218]	N/A	N/A	0.37 [34]	0.27 [26]
	PB-PV-YS	0.37 [34]	0.30 [28]	2.58 [243]	2.10 [198]	N/A	0.72 [68]	0.36 [33]	0.29 [27]
	Average	0.37 [35]	0.29 [27]	2.47 [232]	1.98 [186]	0.67 [63]	0.63 [60]	0.36 [34]	0.28 [26]

Notes. Listed are the critical distances (see Sect. 3 for details) for various cases: four directions for the location of the artificial sources – along the major axis of the beam, along the minor axis, along the jet direction claimed by Li, Morris & Baganoff (2013), and along the one claimed by Yusef-Zadeh et al. (2012); two total flux densities of the artificial sources – 0.2 Jy and 0.55 Jy; and two simple geometries – a single point source and a knotty jet composed of 10 equidistant point-like components. Values outside [inside] brackets are in units of milliarcseconds [Schwarzschild radii]. All values are projected distances.

spatial scales of from sub-mas to a few mas depending on an axis in the geometry of the substructure.

As noted above, the radio flux density that can realistically be attributed to accretion of parts of G2 is $S_{\nu} \approx 0.2$ Jy, translating into a radio luminosity $L_{\rm R} = 4\pi R_0^2 v S_v \approx 1.3 \times 10^{26} \, {\rm W} \approx 0.3 \, L_{\odot}$ (for v = 86 GHz). Without making further assumptions, we can state that this value corresponds to an effective accretion rate $\eta \dot{M} = L_{\rm R}/c^2 \approx 1.5 \times 10^9 \ {\rm kg \ s^{-1}} \approx 7.7 \times 10^{-9} \ M_{\oplus} \ {\rm yr^{-1}},$ with $\eta \in [0,1]$ being the matter-to-light conversion efficiency and c denoting the speed of light. However, in addition we have to take into account that accreted matter might not be converted into electromagnetic radiation but into jets, with the presence of jets being an ad hoc working hypothesis. In this case, a rough quantitative estimate of the accretion rate is provided by the jet power–accretion power relation of radio galaxies: for highly sub-Eddington accretion (as is the case for Sgr A*), kinetic jet power P_{jet} and accretion power $P_{acc} \equiv \dot{M}c^2$ are related like $P_{\rm jet} \approx 0.01 P_{\rm acc}$ (e.g., Allen et al. 2006; Trippe 2014). The powers $P_{\rm jet} \approx 0.017_{\rm acc}$ (e.g., Alich et al. 2000, Hippe 2014). The powers $P_{\rm jet}$ and $L_{\rm R}$ in turn are empirically related like $P_{\rm jet} \approx 5.8 \times 10^{36} (L_{\rm R}/10^{33})^{0.7}$ W (Cavagnolo et al. 2010). Combining the two relations and using, again, $L_{\rm R} \lesssim 0.2$ Jy implies an accretion rate $\dot{M} \lesssim 10^{17}\,{\rm kg\,s^{-1}} \approx 0.5\,M_{\oplus}\,{\rm yr^{-1}}$. We note that this calculation assumes a highly idealized situation, neglecting interactions between G2 and the accretion flow around Sgr A*. Given the small accretion rates as well as the complexity of the accretion flows, it seems realistic that relatively large amounts of matter could be "peeled off" G2 and driven out of the accretion zone by winds or other non-collimated outflows.

These limits on accretion rates, which are always substantially below the total mass of G2 (with details depending on which structure of G2 is assumed), are consistent with the observed kinematics of G2 during its pericenter passage: as noted by several studies, the orbit was purely Keplerian even after the pericenter passage (Witzel et al. 2014; Pfuhl et al. 2015; Valencia-S., et al. 2015). This indicates that G2 did not experience a notable loss of angular momentum and energy, pointing at rather weak interactions with the hot gas around Sgr A*. As suggested by several studies based on hydrodynamical simulations, the viscous timescale can be on the order of years (Burkert et al. 2012; Schartmann et al. 2012; Mościbrodzka et al. 2012), meaning it could take a few more years to see AGN-like (mostly in radio mode associated with hot accretion flows and jets, see Yuan & Narayan 2014 for a review) activity in Sgr A*.

4. Summary and conclusions

We observed Sgr A* with four European GMVA stations at 86 GHz on 1 October 2013, searching for centrally asymmetric (in the observer frame) outflows potentially generated as a consequence of enhanced accretion during the pericenter passage of the gas cloud G2. Our key findings are:

- 1. The closure phases measured for Sgr A* remained zero during the observation time, corresponding to a non-detection (within errors) of asymmetric structure. We are able to constrain the size of the outflows that we could have missed to ≈ 2.5 mas along the major axis and ≈ 0.4 mas along the minor axis of the beam, corresponding to approximately 232 and 35 Schwarzschild radii, respectively. These sizes are on the order of the scale ($\approx 100\,R_{\rm S}$) where magnetically launched AGN jets are supposed to convert magnetic into kinetic energy, but are not yet sufficient to probe structures on scales $\lesssim 10\,R_{\rm S}$ expected in hot accretion flows.
- 2. As probably less than 0.2 Jy of the flux from Sgr A* can be attributed to extra accretion from G2, one finds an effective accretion rate $\eta \dot{M} \lesssim 1.5 \times 10^9 \, \mathrm{kg \, s^{-1}} \approx 7.7 \times 10^{-9} \, M_{\oplus} \, \mathrm{yr^{-1}}$ for material from G2. Exploiting the kinetic jet power–accretion power relation of radio galaxies, one finds that the accretion of matter that ends up in jets is limited to $\dot{M} \lesssim 10^{17} \, \mathrm{kg \, s^{-1}} \approx 0.5 M_{\oplus} \, \mathrm{vr^{-1}}$.

Overall, our analysis suggests that G2 is largely stable against loss of angular momentum and subsequent (partial) accretion at least on time scales $\lesssim 1$ year.

Acknowledgements. We are grateful to Eric W. Greisen (NRAO, U.S.A.) for technical support. We acknowledge financial support from the Korean National Research Foundation (NRF) via Global PhD Fellowship Grant 2014H1A2A1018695 (J.-H. P.) and Basic Research Grant 2012R1A1A2041387 (S. T.). We made use of data obtained with the Global Millimeter VLBI Array (GMVA), which consists of telescopes operated by the MPIfR, IRAM, Onsala, Metsahovi, Yebes and the VLBA. The data were correlated at the correlator of the MPIfR in Bonn, Germany. Last but not least, we are gratful to the anonymous referee for a helpful review and valuable suggestions.

References

Akiyama, K., Kino, M., Sohn, B.-W., et al. 2013, The Galactic Center: Feeding and Feedback in a Normal Galactic Nucleus, Proc. IAU, IAU Symp., 303, 288
Allen, S. W., Dunn, R. J. H., Fabian, A. C., et al. 2006, MNRAS, 372, 21
Anninos, P., Fragile, P. C., Wilson, J., & Murray, S. D. 2012, ApJ, 759, 132

```
Ballone, A., Schartmann, M., Burkert, A., et al. 2013, ApJ, 776, 13
Beckmann, V., & Shrader, C. 2012, Active Galactic Nuclei, Weinheim: Wiley-
Bower, G. C., Falcke, H., Herrnstein, R. M., et al. 2004, Science, 304, 704
Bower, G. C., Goss W. M., Falcke H., et al. 2006, ApJ, 648, L127
Bower, G. C., Markoff, S., Brunthaler, A., et al. 2014, ApJ, 790, 1
Bower, G. C., Markoff, S., Dexter, J., et al. 2015, arXiv:1502.06534v1
Burkert, A., Schartmann, M., Alig, C., et al. 2012, ApJ, 750, 58
Broderick, A. E., Fish, V. L., Doeleman, S. S., & Loeb, A. 2011, ApJ, 738, 38
Brunthaler, A., & Falcke, H. 2013, ATel, 5159, 1
Cavagnolo, K. W., McNamara, B. R., Nulsen, P. E. J., et al. 2010, ApJ, 720, 1066
Chandler, C. J., & Sjouwerman, L. O. 2014, ATel, 6247
De Colle, F., Raga, A. C., Contreras-Torres, F. F., & Toledo-Roy, J. C., ApJ, 789,
   L33
Degenaar, N., Reynolds, M., Miller, J., et al. 2014, ATel, 6458, 1
Falcke, H., Goss, W. M., Matsuo, H., et al. 1998, ApJ, 499, 731
Falcke, H., & Markoff, S. 2000, A&A, 362, 113
Falcke, H., Markoff, S., & Bower, G. C. 2009, A&A, 496, 77
Fish, V. L., Johnson, M. D., Lu, R.-S., et al. 2014, ApJ, 795, 134
Genzel, R., Eisenhauer, F., & Gillessen, S. 2010, Rev. Mod. Phys., 82, 3121
```

Genzel, R., Eisenhauer, F., & Gillessen, S. 2010, Rev. Mod. Phys., 82, 3121
Gwinn, C. R., Kovalev, Y. Y., Johnson, M. D., & Soglasnov, V. A. 2014, ApJ, 794, L14
Gillessen, S., Genzel, R., Fritz, T. K., et al. 2012, Nature, 481, 51
Gillessen, S., Genzel, R., Fritz, T. K., et al. 2013, ApJ, 763, 78
Gillessen, S., Genzel, R., Fritz, T. K., et al. 2013, ApJ, 774, 44
Greisen, E. W. 2003, in Information Handling in Astronomy – Historical Vistas, ed. A. Heck (Dordrecht: Kluwer), Astrophys. Space Sci. Libr., 285, 109
Hada, K., Kino, M., Doi, A., et al. 2013, ApJ, 775, 70
Kamruddin, A. B., & Dexter, J. 2013, MNRAS, 434, 765
Krichbaum, T. P., Graham, D. A., Witzel, A., et al. 1998, A&A, 335, L106
Krichbaum, T. P., Graham, D. A., Bremer, M., et al. 2006, JPhCS, 54, 328
Li, Z, Morris, M. R., & Baganoff, F. K. 2013, ApJ, 779, 154

Liu, H. & Wu, Q. 2013, ApJ, 764, 17 Lo, K. Y., Shen, Z.-Q., Zhao, J.-H., & Ho, P. T. P. ApJ, 1998, 508, L61 Lu, R.-S., Krichbaum, T. P., Eckart A., et al. 2011, A&A, 525, A76 Mahadevan, R. 1997, ApJ, 477, 585 Markoff, S., Falcke, H., Yuan, F., & Biermann, P. L. 2001, A&A, 379, L13 Markoff, S., Bower, G. C., & Falcke, H. 2007, MNRAS, 379, 1519 Melia, F., & Falcke, H. 2001, ARA&A, 39, 309 Miralda-Escudé, J. 2012, ApJ, 758, 86 Mościbrodzka, M., Shiokawa, H., Gammie, C. F., & Dolence, J. C. 2012, ApJ, 752, L1 Narayan, R., Mahadevan, R., Grindlay, J. E., et al. 1998, ApJ, 492, 554 Phifer, K., Do, T., Meyer, L., et al. 2013, ApJ, 773, L13 Pfuhl, O., Gillessen, S., Eisenhauer, F., et al. 2015, ApJ, 798, 111 Schartmann, M., Burkert, A., Alig, C., et al. 2012, ApJ, 755, 155 Scoville, N., & Burkert, A. 2013, ApJ, 768, 108 Shepherd, M. C. 1997, in Astronomical Data Analysis Software and Systems VI, eds. G. Hunt, & H. E. Payne (San Francisco: ASP), ASP Conf. Ser., 125, 77 Shen, Z.-Q., Lo, K. Y., Liang, M.-C., et al. 2005, Nature, 438, 62 Thompson, A. R., Moran, J. M., & Swenson, G. W. Jr. 2001, Interferometry and Synthesis in Radio Astronomy. New York: Wiley. 2nd ed. Trippe, S. 2014, JKAS, 47, 159 Valencia-S., M., Eckart, A., Zajaček, M., et al. ApJ, 800, 125 Witzel, G., Ghez, A. M., Morris, M. R., et al. 2014, ApJ, 796, L8 Yuan, F., Markoff, S., & Falcke, H. 2002, A&A, 383, 854 Yuan, F., Quataert, E., & Narayan, R. 2003, ApJ, 598, 301 Yuan, F., & Narayan, R. 2014, ARAA, 51, 529 Yusef-Zadeh, F., Arendt, R., Bushouse, H., et al. 2012, ApJ, 758, L11 Zajaček, M., Karas, V., & Eckart, A. 2014, A&A, 565, A17 Zylka, R., Mezger, P. G., & Lesch, H. 1992, A&A, 261, 119